CILAMCE 2017

Florianópolis - Santa Catarina - Brazil

ANALYSIS OF A FRAMED STRUCTURE CONSIDERING THE SSI AND SUBJECTED TO DYNAMIC WIND LOAD.

Eduardo Assad Kaba Naccache

eduardo.naccache@usp.br, PhD student at University of São Paulo

Av. Prof. Almeida Prado tv. 2, n. 83, 05508-070, São Paulo, SP, Brazil

Valério Silva Almeida

valerio.almeida@usp.br, professor at University of São Paulo

Av. Prof. Almeida Prado tv. 2, n. 83, 05508-070, São Paulo, SP, Brazil

Abstract. *As another improvement in the structural analysis, a different way of soil structure interaction (SSI) is proposed for pile groups foundations. The pile-soil interaction is peculiar and yields a valuable settlement assess of the corresponding supported superstructure. An also peculiar combination with a dynamic synthetic wind technique permits a SSI analysis for dynamic wind loads. The possible influences that the SSI do at the horizontal displacement at the top is investigated. Some issues arise like whether some imposed limit horizontal displacement remains coherent if the SSI is taken under consideration.*

Keywords: *Dynamics, Finite element method, Boundary element method, Soil structure interaction.*

1 INTRODUCTION

The structural behavior of a building is governed, among other things, by the interaction between the superstructure (that part of the building which accommodates useful environment), the infrastructure (that part of the building which transfers its loads to the soil) and the soil. Nevertheless, the design common practice does not take this complete interaction into consideration; the superstructure is assumed resting on fixed supports and the foundations are dimensioned with this fixed support reactions. At present time, more efforts are needed to make the soil structure interaction analysis a more viable and common practice and so, one needs to exploit the potentialities of the many possible ways to model this interaction, as with the Winkler hypothesis applied by an uncountable number of authors and which substitutes the whole soil mass by groups of discrete or continuous springs. Among several other methodologies to model the soil structure interaction, there are those of the elasticity theory found in the works of Poulos (1967), Burmister (1945), Chan *et al.* (1974), Davies and Banerjee (1978); those that makes use of the Finite Element Method (FEM), as in the works of Ottaviani (1975) and Chow and Teh (1991); those that makes use of the Finite Layer Method (FLM), as in the works of Southcott and Small (1996) and Ta and Small (1998); those that makes use of the Boundary Element Method (BEM), as in the works of Banerjee (1976), Banerjee and Davies (1977) and Maier and Novati (1987).

In this work, the soil structure interaction makes use of the Winkler hypothesis, the FEM and of the BEM at once. The piles are finite elements coupled with the load lines inside the soil mass represented by a semi-infinite homogenous medium. A non-linear behavior is introduced as the slip between the pile and the soil is permitted and happens when the shear stresses on the interface grows beyond the limit shear stress of the adherence model (Naccache, E. A. K., 2017). A decoupled interaction is defined with the framed structure and the horizontal displacement at the top is analyzed supposing a static equivalent wind action and a dynamic synthetic wind action.

2 FOUNDATION MODEL

The framed structure under consideration is supported by piles groups. It constitutes an independent soil-structure interaction model which are used to calculate the basement displacements. The soil is represented by a homogenous semi-infinite medium given by the Mindlin fundamental solution in association with the Somigliana identity and each pile are represented by a finite element with four nodes and fourteen degrees of freedom (Figure 2(a)). The resultant equation of the BEM-FEM coupling considering the pile-soil slip is:

$$\left(\mathbf{K}_{piles}+\mathbf{M}_{soil}\right)\mathbf{U}_{piles}+\mathbf{K}_{s,piles}\mathbf{d}_{p-s}=\mathbf{f}_{piles} \tag{1}$$

Where $\mathbf{K}_{pile}$ is the piles stiffness contribution; $\mathbf{M}_{soil}$ is the soil stiffness contribution; $\mathbf{U}_{pile}$ is the piles nodal displacements under pile-soil adherence existence; $\mathbf{K}_{s,pile}$ is the piles

Proceedings of the XXXVIII Iberian Latin-American Congress on Computational Methods in Engineering
P.O. Faria, R.H. Lopez, L.F.F. Miguel, W.J.S. Gomes, M. Noronha (Editores), ABMEC, Florianópolis, SC, Brazil, November 5-8, 2017.

stiffness under pile-soil slip; $\mathbf{d}_{p-s}$ is the piles slip; $\mathbf{f}_{pile}$ is the pile head load from the frame superstructure.

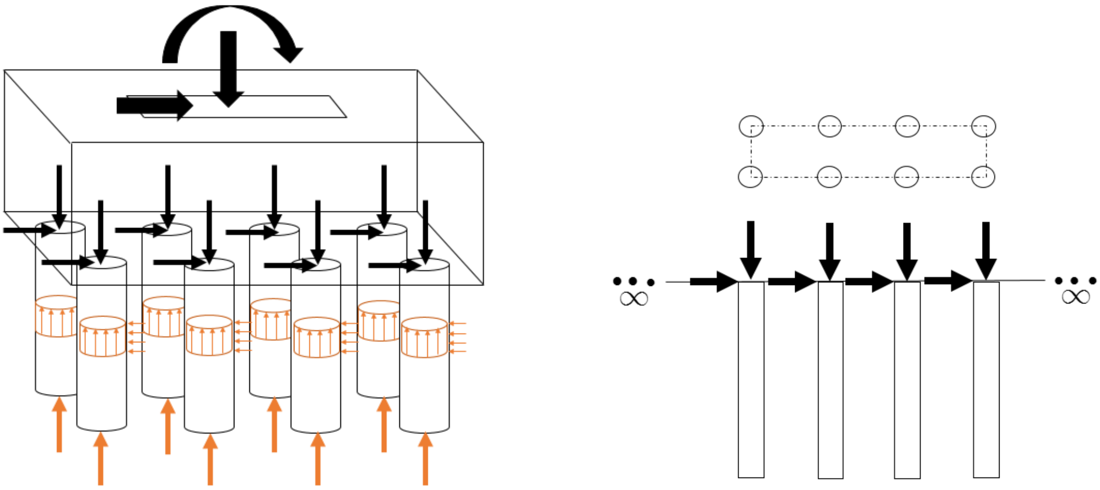

(a) (b)

Figure 1. Load path from columns to piles (a). Foundation BEM-FEM model (b).

The slip between the pile and the soil is governed by a friction coefficient evolution function that gives the mobilized friction coefficient μ on the pile-soil interface (De Gennaro; Frank, 2012):

$$\mu(w_t) = \begin{cases} \mu_0 + (\mu_p - \mu_0)\dfrac{w_t}{A\left(\dfrac{\sigma_{ni}}{p_0}\right)t + \mu_t}, & if \quad w_t \le w_{tf} \\ \mu_r + (\mu_p - \mu_r)\dfrac{1}{\cosh\left[\dfrac{A_0}{t}(w_t - u_{tf})\right]}, & if \quad w_t > w_{tf} \end{cases} \tag{2}$$

Where w_t is the relative tangential displacement; w_{tf} is relative tangential displacement at peak friction; μ_r is the friction coefficient at failure; μ_0 is the friction coefficient delimiting the initial elastic region; μ_p is the peak friction coefficient; is the thickness of the interface layer; A and A_0 are parameters that defines the shape of the function; p_0 is a reference pressure ensuring a dimensionless expression.

If the shear tension on the interface surpass the limit given by:

$$\tau_{\lim} = \mu(w_t)\sigma_v K_0 \tag{3}$$

a soil independent displacement is observed and accumulated in $\mathbf{d}_{p-s}$. (σ_v is the vertical stress for a correspondent soil layer and K_0 is the lateral earth pressure coefficient.)

At each node, the total pile displacement value is (Figure 2):

$$w_p = w_s + w_{p-s} \tag{4}$$

Where w_s is the displacement parcel for which the soil moves together with the pile and w_{p-s} is the pile-soil slip (Figure 2).

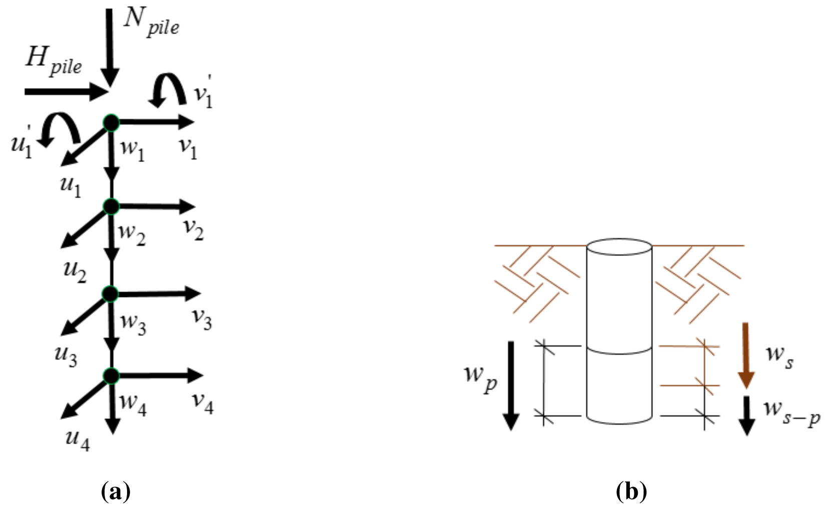

Figure 2. Pile finite element with the only two external loads applied by the framed structure (a). Pile total vertical displacement (b).

More details about the BEM-FEM model used here for the piles immersed in a homogeneous soil are found in Naccache, E. A. K. (2016).

3 FRAME MODEL

The frame model is linear elastic with Bernoulli-Euler bar elements. The connections between the bars are rigid and the frame structure is not coupled with the foundations presented above. The frame and foundation interaction is described in the following topic.

The Bernoulli-Euler bar element is well known of the engineering community. When the shear deformation is ignored and the cross section is assumed rigid and without relative rotation respect its longitudinal axe, its cinematic rules are established. In a finite element approach the exact result of the Bernoulli-Euler theory is achieved when adopting third order polynomials for the displacement shape functions.

In a dynamic analysis, the mass properties of a structure must be considered. There are basically two ways to do it. Slumped masses can be strategically positioned to represent the whole structure mass or a density function can be used to represent the mass distribution throughout the bar. For a uniform mass distribution $\bar{m}$, the resultant mass matrix is:

$$\mathbf{M}_e = \frac{\bar{m}l}{420}\begin{bmatrix} 140 & 0 & 0 & 70 & 0 & 0 \\ 0 & 156 & 22l & 0 & 54 & -13l \\ 0 & 22l & 4l^2 & 0 & 13l & -3l^2 \\ 70 & 0 & 0 & 140 & 0 & 0 \\ 0 & 54 & 13l & 0 & 156 & -22l \\ 0 & -13l & -3l^2 & 0 & -22l & 4l^2 \end{bmatrix} \quad (5)$$

For the structural damping, a Rayleigh proportional damping is adopted. The damping matrix is a linear combination of the mass and stiffness matrixes, that is:

$$\mathbf{C}_{Rayleigh} = a_0\mathbf{M} + a_1\mathbf{K} \quad (6)$$

To determinate the coefficients a_0 and a_1 it is sufficient to set the viscous damping rate for only two modes of vibration.

The program used for the generation and analysis of the framed structure is PORTICO2D and was developed by the authors. He permits the user to choose the number of floors (npav), each one with a different height and the number of bays (nv), each one with a different length.

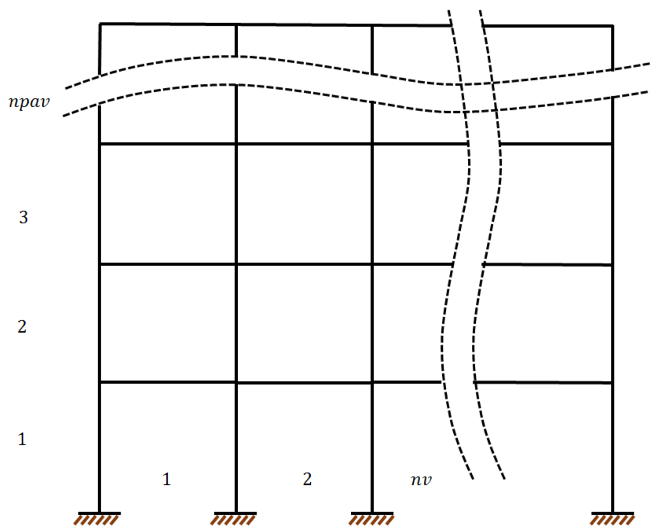

Figure 3. Framed structure generated by PORTICO2D.

4 FRAME AND FOUNDATION INTERACTION

In regards of the soil structure interaction through the pile foundation, it is not a coupled interaction as was already stated. First the support reactions are obtained and then applied at the piles heads. The vertical and horizontal piles heads displacements are used to get the equivalents coefficients of subgrade reactions k_v, k_h and k_φ, by the following expressions:

$$k_v = \frac{n\,N_{col}}{\left(\sum_{i=1}^{n} w_i\right)} \tag{7.1}$$

$$k_h = \frac{n\,H_{col}}{\left(\sum_{i=1}^{n} v_i\right)} \tag{7.2}$$

$$k_\varphi = \frac{l_{de}\,M_{col}}{\left(\sum_{i=1}^{nd} \left|w_{i,\mathrm{d}}\right| - \sum_{i=1}^{ne} \left|w_{i,\mathrm{e}}\right|\right)} \tag{7.3}$$

Where H_{col} and N_{col} are respectively the horizontal and vertical action from the columns and l_{de} is the distance between two consecutive piles. These coefficients are added to the frame stiffness matrix.

5 WIND LOAD

5.1 Fluctuating component

Franco (1993) proposed a new technique to represent the wind fluctuating component based on Davenport's power spectrum. The fluctuating parcel of the wind pressure was assumed to be proportional to mean wind (measured in 10 min or 1-hour interval) and peak wind (measured in 3 to 5s interval) velocity ratio. If the height is not considered, this ratio is:

$$\frac{q_{600}}{q_3} = \left(0,69\right)^2 = 0,48 \tag{8}$$

The power spectrum of the wind is a function of the height z and the frequency f. It shows the range of frequencies that the wind can develop when blowing and the relative importance of each strip of frequencies. The logarithmical frequency scale is commonly used, then, for convenience, a reduced power spectrum S_r is defined:

$$S_r\left(z,f\right) = \frac{f\,S\left(z,f\right)}{v_*^2} = \frac{4x^2}{\left(1+x^2\right)^{4/3}} \qquad x = \frac{1220 f}{V_0} \tag{9}$$

The technique necessary to obtain the time functions that represent the wind fluctuating components consists in combine the properties of the Davenport's power spectrum with a Fourier integral, which applies to general non-periodic loads. A complete Fourier integral (or Fourier transform) is an improper integral given by:

$$p(t)=\int_{-\infty}^{\infty} C(f)\cos\left[2\pi f t-\theta(f)\right]df \tag{10}$$

Where,

$$a(f)=\int_{-\infty}^{\infty} p(t)\cos(2\pi f t)\,dt \tag{11}$$

$$b(f)=\int_{-\infty}^{\infty} p(t)\mathrm{sen}(2\pi f t)\,dt \tag{12}$$

$$C(f)=\sqrt{a^2(f)+b^2(f)} \tag{13}$$

$$\theta(f)=\tan^{-1}\frac{b(f)}{a(f)} \tag{14}$$

The variance of a function $x(t)$ is:

$$\sigma^2\left[x(t)\right]=\frac{1}{T}\int_0^T\left[x(t)-\overline{x}\right]^2 dt \tag{15}$$

The mean value of the fluctuating wind is zero, then its variance is:

$$\begin{aligned}\sigma^2\left[p(t)\right]&=\frac{1}{T}\int_0^T p^2(t)\,dt=\frac{1}{T}\int_0^T\int_{-\infty}^{\infty} C^2(f)\cos^2\left[2\pi f t-\theta(f)\right]df\,dt\\&=\int_{-\infty}^{\infty}\frac{1}{T}\int_0^T C^2(f)\cos^2\left[2\pi f t-\theta(f)\right]dt\,df\\&=\frac{1}{2}\int_{-\infty}^{\infty} C^2(f)\,df\end{aligned} \tag{16}$$

There is a relation between the variance and de power spectrum, that is:

$$\sigma^2\left[p(t)\right]=\int_0^{\infty} S(f)\,df \tag{17}$$

Equations (16) and (17) can be equaled, yielding:

$$C(f)=\sqrt{2S(f)} \tag{18}$$

Proceedings of the XXXVIII Iberian Latin-American Congress on Computational Methods in Engineering
P.O. Faria, R.H. Lopez, L.F.F. Miguel, W.J.S. Gomes, M. Noronha (Editores), ABMEC, Florianópolis, SC, Brazil, November 5-8, 2017.

Using equation (10) an infinite number of harmonic function would be included but, accordingly with Franco (1993), only eleven ones are sufficient if conveniently chosen in a way that their periods can cover all the spectrum interval, that is:

$$p(t) \cong \sum_{k=1}^{11} C_k \cos\left(\frac{2\pi}{T_r r_k} t - \theta_k\right) \tag{19}$$

$$r_k = 2^{k-r} \tag{20}$$

The phase angles θ_k are undetermined, their values are randomly chosen.

The amplitude of each of the eleven harmonic functions are a proportional parcel of the total fluctuating pressure, as follows:

$$p_k = \frac{C_k}{\sum_{k=1}^{11} C_k} p = c_k p \tag{21}$$

Franco punctuate that with eleven harmonic functions the contribution of the resonant component is overestimated by a factor of 2, then the coefficients c_k are corrected dividing the resonant component by 2 and adding the remaining of the resonant coefficient in the adjacent coefficients:

$$c^*_{k\,res} = \frac{c_{k\,res}}{2} \tag{22.1}$$

$$c^*_{kres-1} = c_{kres-1} + \frac{c_{kres}}{4} \tag{22.2}$$

$$c^*_{kres+1} = c_{kres+1} + \frac{c_{kres}}{4} \tag{22.3}$$

The last concept needed to implement the technique is the spatial correlation of velocities and pressures of the wind fluctuating components. The grater the distance from the gust center, the lesser the correlation coefficient. The correlation function is given by (Franco, 1993):

$$Corr(\Delta z, f_k) = \exp\left(-\frac{7\Delta z\, f_k}{V_0}\right) \tag{23}$$

An equivalent perfectly correlated gust can be defined and its height is (Franco, 1993):

$$\Delta z_{0k} = \frac{V_0}{7 f_k} \tag{24}$$

This height is used to define two triangles of base 1 and height Δz_{0k} to create an equivalent linear decay of the of the exponential spatial correlation given in equation (23).

The gust center was determined with and optimization solver that permitted to find the position of maximum bending moment of the resonant component.

5.2 Constant component

The total wind pressure q that act on the structure follows the proceedings of the NBR 6123:1988 which stablish that:

$$q = 0{,}613 V_k^2 \tag{25}$$

$$V_k = S_1 S_2 S_3 V_0 \tag{26}$$

The constant parcel q_{const} of q is obtained when the coefficients of the S_2 factor corresponds to mean speed velocity measures with time intervals of 10 minutes to 1 hour. The remaining parcel of the total pressure after subtracting q_{const} from q is the total fluctuating parcel:

$$q_{fl} = q - q_{const} \tag{27}$$

The final wind load applied at each j floor of the structure becomes:

$$F_j = C_a A_{ej} \left[\sum_{i=1}^{11} c_{ki} Corr_{ji}\, q_{flj} \cos\left(\frac{2\pi}{T_r r_i} t - \theta_i \right) + q_{constj} \right] \tag{28}$$

6 EXAMPLE

The following example is a concrete thirty-two floors and 4 bays framed structure, with hundred and two point four meters height, thirty-two meters length and thirty-six meters width. The wind influence width is eight meters.

The extreme columns are supported by groups of four piles 80 centimeters diameter and 22 meters length. The intermediate columns are supported by groups of eight piles 80 centimeters diameters and 20 meters length. Inside each pile group, 2 meters is the distance between the piles. The Young elastic modulus of piles concrete is 23,8GPa. The soil parameters are resumed in Table 1.

The structural viscous damping ratio is $\xi = 0{,}05$. The soil damping is neglected as this work represent only the authors initial incursions on the matter, letting this considerations for futures works.

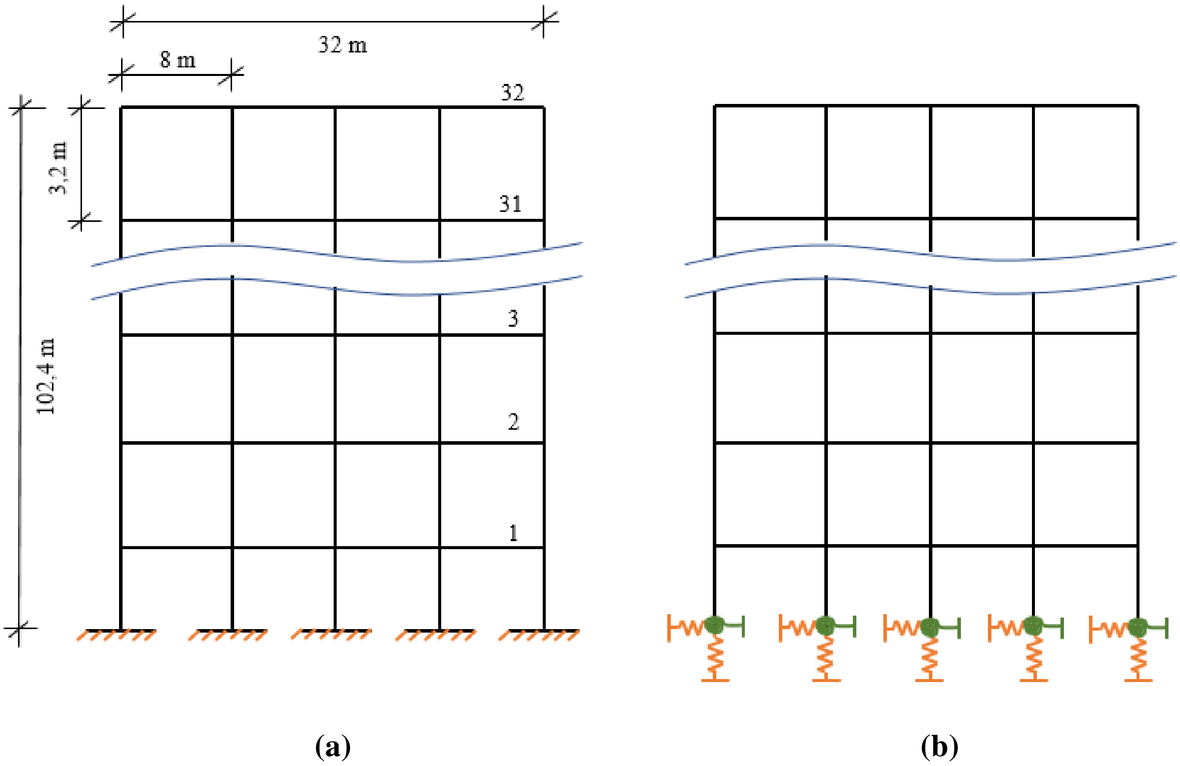

Figure 4. Example framed structure with rigid foundation (a). Example framed structure with elastic foundations (b).

The Young elastic modulus of the structure is 30 GPa. The columns are 225 centimeters length and 30 centimeters width. The beams are 75 centimeters height and 30 centimeters width. The total vertical load applied along the beams is 80kN/m.

Soil Parameters									
E_S	ν	μ_0	μ_r	μ_p	A	A_0	t	u_{tf}	σ_{ni}/p_0
80,0 Mpa	0,3	0,0	0,58	0,68	0,00008	15,0	3 mm	1 mm	1,0

Table 1. Soil parameters for the BEM-FEM foundation model.

The location of the possible tower is São Paulo city, this city is positioned on a region of the wind design chart of around 39 m/s for the basic wind speed. The wind design chart used here is an actualization of that one still current in the Brazilian standards and is found in the work of Beck and Corrêa (2012). The S_1 factor and the S_3 factor are both 1,0. The building class is C and the building category is V (NBR 6123:1988). The total wind pressure is then calculated for time intervals of 10 seconds. The mean wind pressure is calculated for time intervals of 10 minutes. The needed parameters to calculate the S_2 factor are in Table 2.

S2					
Total wind			Constant wind		
b	p	Fr	b	p	Fr
0,71	0,175	0,95	0,5	0,31	0,69

Table 2. S2 wind factor.

Only the drag coefficient C_a remains undetermined. For a high turbulence wind zone, $C_a = 1{,}0$ or for a low turbulence wind zone, $C_a = 1{,}3$. As observed, there is a great difference at the wind forces if the drag coefficient is not correctly chosen. The two situations will be examined for better understanding of this issue.

In the static analysis, the influence of the turbulence type was compared in Figure 5. Note that the SSI is considered and after ignored for each turbulence type. The horizontal displacement at the top were 5,82 cm, 7,28 cm, 7,56 cm, 9,32 cm for each case and in the same order of that displaced in Figure 5.

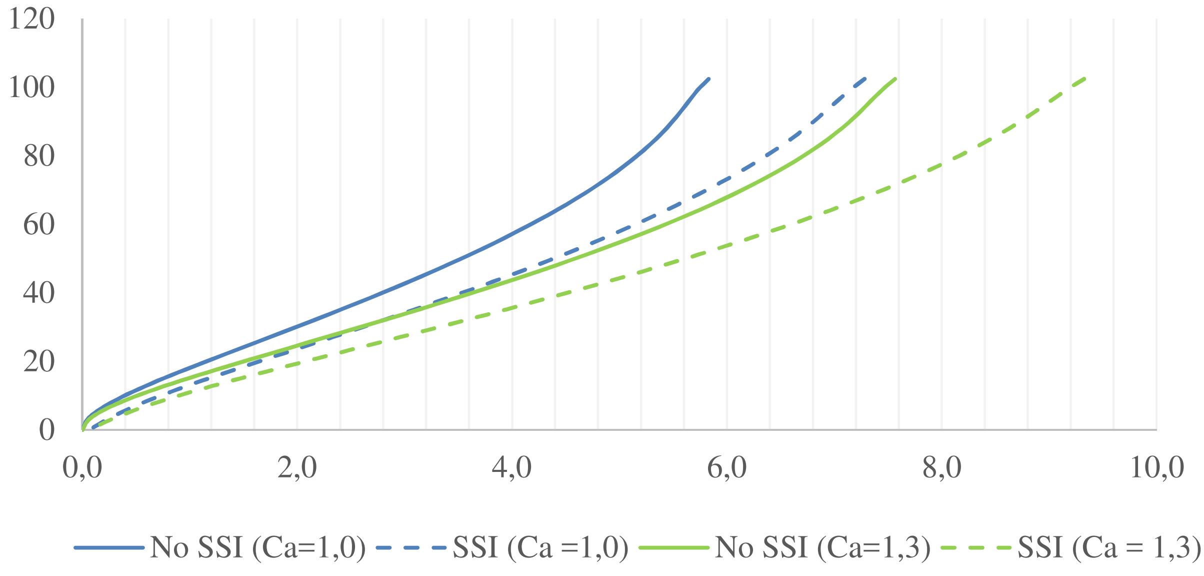

Figure 5. Horizontal displacement profile. Static wind.

In the dynamic analysis, four different situations were considered too but only with one value for the drag coefficient which was chosen to be 1,3. First ignoring the SSI, twenty loads combinations were generated for an undamped framed structure and a damped framed structure. The maximum displacements values for each combination formed a Gumbel probability distribution and a characteristic displacement value was stablished for a 5%

probability of being exceeded. These characteristic combinations were plotted in Figure 6(a) and its maximum displacements were 7,96 cm for $\xi = 0,05$ and 9,16 cm for $\xi = 0,0$. More two situations were generated by considering the SSI. The same proceedings were followed and the characteristic combinations were plotted in Figure 6(b). The maximum displacements were 24,0 cm for $\xi = 0,05$ and 29,6 cm for $\xi = 0,0$. The Newmark numerical integration method was used.

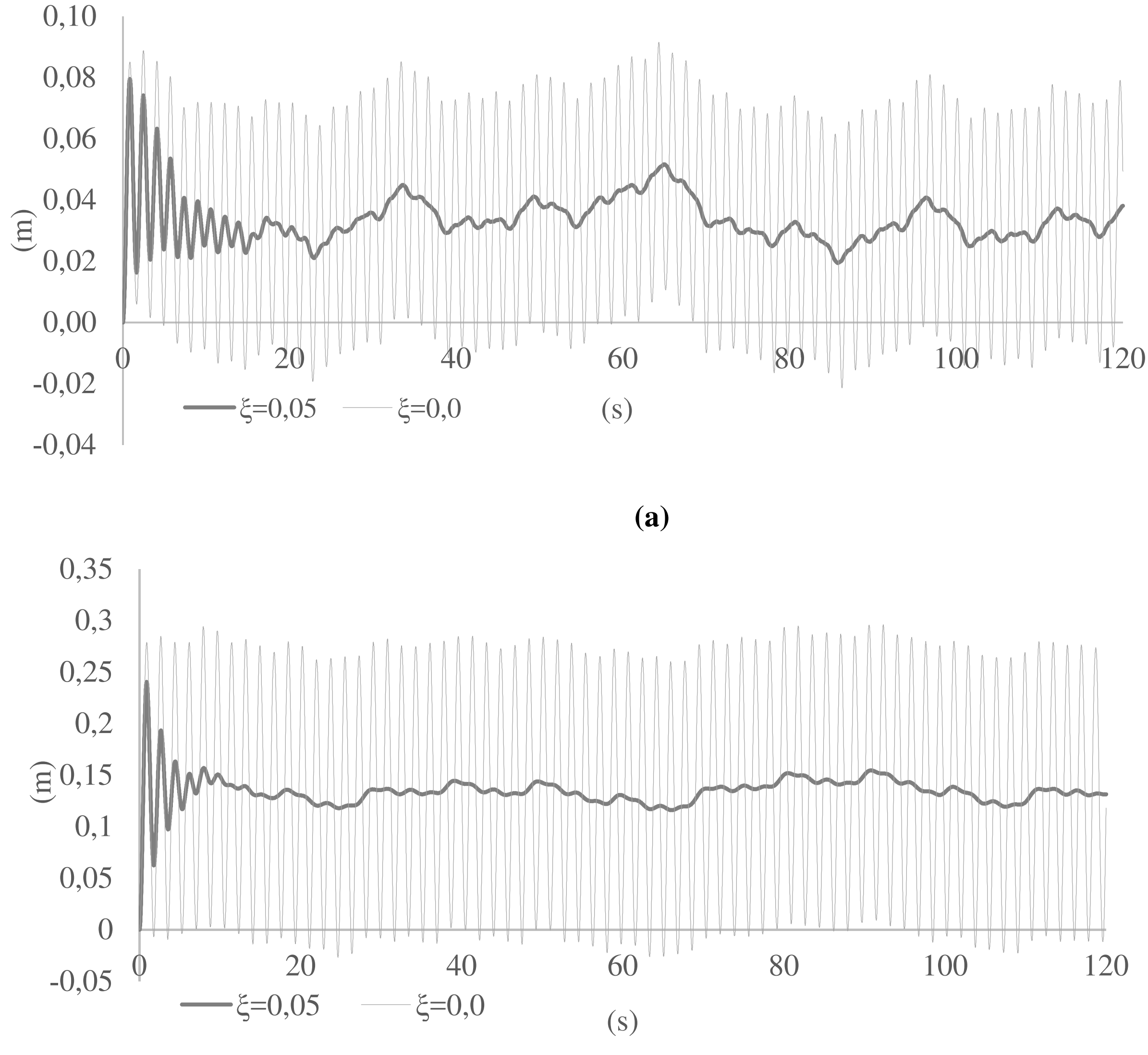

(a)

(b)

Figure 6. Horizontal displacement at the top for the synthetic dynamic wind. Without the SSI (a). With the SSI (b).

Proceedings of the XXXVIII Iberian Latin-American Congress on Computational Methods in Engineering
P.O. Faria, R.H. Lopez, L.F.F. Miguel, W.J.S. Gomes, M. Noronha (Editores), ABMEC, Florianópolis, SC, Brazil, November 5-8, 2017.

7 CONCLUSIONS

In this work, a structural analysis of a framed structure resting on pile foundations was presented. The pile soil interaction is a non-linear model not commonly applied in the SSI analysis. The synthetic dynamic wind method used is an important current available method that permits one to assess the dynamic behavior of tall buildings due to wind action.

A brief study pointed out the great importance of a correct characterization of a building vicinity as it influences the wind turbulence type which is responsible for great differences on the wind forces that act on the structure and the correspondent horizontal displacements as shown in Figure 5.

According to the maximum displacements obtained in the static and dynamic analysis of Figures 5 and 6, it is evident that the SSI may cause a non-neglectable influence on the horizontal displacement of a tall building (At least when it is modeled as a framed structure). The natural consequences are that in some situations the preconized limit horizontal displacement permitted by a code would not be respected if the SSI takes place in a building previously designed with fixed foundations.

The structural damping takes around 10 seconds to show its effects on the structure, then not sufficient fast for the gust blow lasts this same time interval. The structural damping should act more rapidly if to soften the dynamics effects. On the other hand, if a longer time interval could be permitted as representative, the maximum displacement would be around 14,0 cm (Figure 6(b)) not so different from that obtained in the static analysis considering the SSI, which was 9,32 cm.

ACKNOWLEDGEMENTS

The authors would like to thank the academic support given by the PPGEC-EPUSP (Programa de Pós-Graduação em Engenharia Civil da Escola Politécnica da Universidade de São Paulo) and the financial support of CAPES (Coordenação de Aperfeiçoamento de Pessoal de Nível Superior) and Cnpq (Consenlho Nacional de Desenvolvimento Científico e Tecnológico).

REFERENCES

Almeida V.S., Paiva J. B., 2004. A mixed BEM-FEM formulation is layered soil-superstructure interaction. *Engineering Analysis with Boundary Elements,* v. 28, pp. 1111-1121.

Almeida V.S., Paiva J. B., 2007. Static analysis of soil/pile interaction in layered soil by BEM/BEM coupling. *Engineering Analysis with Boundary Elements*, v. 38, pp.835-845.

Banerjee P. K., 1976. Integral equation methods for analysis of piece-wise nonhomogeneous three-dimensional elastic solids of arbitrary shape. *Int. J. Mechanical Science*, v.18, pp.293-303.

Banerjee P.K., Davies T.G., 1977. Analysis of pile groups embedded in Gibson soil. *In: Int. Conf. Soil Mechs Fdn Engng., 9th, Tokyo. Proc.*, v. 1, pp.381-386.

Beck, A. T., Carrêa, M. R. S., 2013. New Design Chart for Basic Wind Speeds in Brazil. *Latin American Journal of Solids and Structures*, v. 10, pp 707-723.

Chan K. S., Karasudhi P., Lee S. L., 1974. Force at a point in the interior of a layered elastic half-space. *Int. J. Solids Structs.,* v. 10, pp. 1179-99.

Chow Y. K., Teh C. I., 1991. Pile-cap-pile-group interaction in nonhomogeneous soil. *Journal of Geotechnical Engineering*, v. 117, pp. 1655-1668

Corelhano, A. G. B., Corrêa, M. R. S., Beck, A. T., 2012. Reliability of buildings in service limit state for maximum horizontal displacements. *Ibracon structures and materials journal*, v.5, pp. 84-103.

Davies T. G., Banerjee P. K., 1978. The displacement field due to a point load at the interface of a two-layer elastic half-space. *Géotechnique,* v. 28, pp. 43-56.

De Gennaro, V., Frank, R., 2002. Elasto-plastic analysis of the interface behavior between granular media and structure. *Computers and Geotechnics*, v. 29, pp. 547-572.

Franco, M., 1993. Direct Along-Wind Dynamic Analysis of Tall Structures. *Technical bulletin of the Polytechnic school of University of São Paulo*, v. 9303, 22p.

Maier G, Novati G., 1987. Boundary element elastic analysis by a successive stiffness method. *Int. J. for Numerical and Anal. Methods in Geomechanics*, v. 11, pp. 435-47.

Naccache, E. A. K., 2017. Confiabilidade de estacas. *Novas edições acadêmicas*. Saarbrücken, Deutschland.

NBR6123:1988: Wind Loads in Buildings. ABNT – Brazilian Association of Technical Codes, Rio de Janeiro.

Ottaviani M., 1975. Three-dimensional finite element analysis of vertically loaded pile groups. *Géotechnique*, v. 25 (2), pp. 159-174.

Poulos H. G., 1967. Stresses and displacements in an elastic layer underlain by rough rigid base. *Géotechnique*, v. 17, pp. 378-410.

Ribeiro, D. B, Paiva, J. B., 2014. A new BE formulation coupled to the FEM for simulating vertical pile groups *Engineering Analysis with Boundary Elements,* v. 41, pp.1–9.

Southcott P. H., Small J. C., 1996. Finite layer analysis of vertically loaded piles and pile groups. *Computer and Geotechnics*, v. 18, pp. 47-63.

Ta L. D., Small J. C., 1998. Analysis and performance of piled raft foundations on layered soils-case studies. *Soil and Foundations*, v. 38 (4), pp. 145-150.

Tabatabaiefar, S. H. R.; Fatahi, B.; Samali, B. (2013). Seismic behavior of building frames considering dynamic soil-structure interaction. Int. J. Geomechanics, v.13(4), pp.409-420.

Wilson, E. L. Three-Dimensional Static and Dynamic Analysis of Structures. *Computers and Structures Inc*. Berkeley, California, 2002.